ISSN 1560-0904, Polymer Science, Series B, 2022, Vol. 64, No. 4, pp. 546–552. © Pleiades Publishing, Ltd., 2022.
ISSN 1560-0904, Polymer Science, Series B, 2022. © Pleiades Publishing, Ltd., 2022.

COMPOSITES

Enhancing Glass Transition Temperature of Poly(methylmethacrylate) by Incorporating Methacrylate-Functional Silane Grafted SiO_2 Nanoparticles

Emre Yavuz[a,b], Ramazan Erdem[c,*], and Esin Akarsu[b]

[a] *Department of Civil Engineering-Construction Materials, Institute of Science, Akdeniz University, Antalya, 07058 Turkey*
[b] *Department of Chemistry, Akdeniz University, Institute of Science, Antalya, 07058 Turkey*
[c] *Department of Textile Technologies, Serik GSS Vocational School of Higher Education, Akdeniz University, Antalya, 07500 Turkey*
**e-mail: ramazanerdem@akdeniz.edu.tr*

Received January 29, 2022; revised April 25, 2022; accepted May 20, 2022

Abstract—Nanocomposites attract the attention of researchers due to the increasing demand on materials having unique properties. Incorporation of nanoparticles into polymers considerably improves some materials properties such as thermal stability. In current study, PMMA/SiO_2 hybrid nanocomposites including ungrafted and grafted silica nanoparticles have been prepared. The surfaces of SiO_2 nanoparticles were grafted with 3-(methacryloyloxypropyl)trimethoxysilane (MPTS) and 3-(methacryloyloxypropyl)triethoxysilane (MPTES) by sol-gel technique. The structure, morphology and thermal properties of the obtained bulk materials were investigated by FTIR, SEM-EDX, TGA and DSC. Based on the studies of infrared spectroscopy, polymerization of MMA monomers was approved by following the intensity of acrylate group. Thermal characteristics of nanocomposite structures enhanced remarkably as SiO_2 nanoparticles were introduced to the polymer matrix and glass transition temperature T_g value reached to the highest (166°C) for MPTES@20% SiO_2-PMMA hybrid nanocomposite. According to SEM analysis, the most homogenous structure belonged to MPTES@20% SiO_2-PMMA hybrid nanocomposite.

DOI: 10.1134/S1560090422700191

INTRODUCTION

Polymer based composites are advantageous materials in many areas due to their satisfactory mechanical properties and low cost availability. They are widely utilized in various emerging fields of automotive, aerospace, coatings, sensors, organic light emitting diodes, solar cells, adhesives, fire retardants, packaging materials, microelectronics, drug delivery, membranes and medical devices [1–5]. The characteristics of polymer based composites are mainly influenced by their structures, polymerization technique, modification and organic or inorganic filler they contain [6].

Poly(methylmethacrylate) (PMMA) is one of the most widely used synthetic polymers, which has been the focus of the scientific world in recent years due to its versatile features in terms of good weatherability, high strength, excellent dimensional stability, reduced gas permeability, improved physical performance and increased heat resistance [6–8]. To emphasize that having a good thermal stability and super optical clarity, PMMA is especially very useful in applications where light transmission is important [9, 10].

Recently, significant efforts have been made to elaborate and develop organic/inorganic (hybrid) nanocomposite materials [11, 12]. By incorporating nanoparticles into organic materials, it is possible to obtain structures with significantly improved characteristics. Hybrid composite materials can be examined in two different categories depending on the structure and phase bond. In the first category, the inorganic component is simply distributed in the matrix and there exist only weak physical interactions between the two phases, such as hydrogen bonding or Van der Waals forces. In the second category, hybrids can be obtained creating stronger structures by forming strong chemical interactions (grafting) such as covalent bonds between the components [13, 14]. Grafting of inorganic nanoparticles could be an appropriate alternative to establish strong chemical interactions as well as to enable cross-linking between inorganic nanoparticles and organic polymeric matrix. Grafting mechanism generally occurs between OH groups of nanoparticles and functional groups of some specific complexes such as silane halides and alkoxides, phosphonates, carboxylates, catechols and amines, etc. Furthermore, surface modification also plays an important role for stabilizing nanoparticles in the solution to prevent them from coalescing, agglomerat-

ing, or aggregating-which may unfavorably influence their properties and application [15–19].

The synthesis of PMMA doped with SiO_2 hybrid-nanocomposites have been drawn much attention in the research field. One of the reasons for that is the increment in glass transition temperature T_g of the hybrid nanocomposite due to the SiO_2 role of increasing physical interactions within the polymer matrix which leads slower relaxation process as a result of the immobilization and restriction of polymer segments [20–22]. In order to shift the T_g of eventual hybrid nanocomposite to much higher point, grafting of SiO_2 nanoparticles could be an option. Regarding this issue, several studies have been reported in the literature, for instance; Hu et al. prepared PMMA/silica nanocomposites by grafting the surface of silica nanoparticles with two methyl, three methyl and one octane functional silanes separately. When the 4 wt % of grafted SiO_2 particles were introduced to the blend, the T_g of PMMA/silica was shifted from 113 to 125°C, 126 and to 131°C, subsequently [23]. Salami-Kalajahi et. al. recorded that the synthesis of PMMA/SiO_2 was carried out by incorporating 7 wt % of surface grafted silica nanoparticles with3-methacryloxypropyldimethylchlorosilane. Results exhibited that T_g values of PMMA/SiO_2 varied from 79.8 to 102.1°C [24]. Lin et al. synthesized SiO_2 nanoparticles by utilizing Stöber method [25] and grafted them with 3-(methacryloyloxy)propyl trimethoxysilane (MPTS). Finally, films containing PMMA/SiO_2 were obtained. According to the findings, T_g of pure PMMA was recorded as 94°C and increased to 101°C as grafted silica nanoparticles incorporated into the PMMA [26].

While various preparation methods of PMMA/silica hybrid nanocomposites such as bulk polymerization [23], emulsion polymerization [27, 28], micro emulsion polymerization [11], solution polymerization [29], sol–gel method [30] have already been intensively explored in the literature, the universal behavior in terms of the impacts of grafted silica nanoparticles on T_g and the relaxation dynamics of PMMA polymer chains have not yet been exactly proved.

The aim of this current study is to prepare PMMA/SiO_2 hybrid nanocomposites and investigate the alterations of T_g values of the prepared structures. First of all, in order to ensure an effective bonding between polymer matrix and nanoparticles, the surfaces of SiO_2 nanoparticles were grafted with polimerizable groups of 3-(methacryloyloxypropyl)trimethoxysilane (MPTS) and 3-(methacryloyloxypropyl)triethoxysilane (MPTES) by sol–gel technique. Afterwards, PMMA/SiO_2 hybrid nanocomposite synthesis was realized through radical polymerization. Ultimately, the properties of obtained nanocomposite structures were characterized by FTIR, DSC, TGA and SEM-EDS analyses.

EXPERIMENTAL

Materials

Methyl methacrylate (MMA) (Sigma-Aldrich, 99%), benzoyl peroxide (BPO) (Sigma-Aldrich, 75%) were used as monomer and thermal initiator, respectively. Organosilicasol (10–15 nm, 30–31% SiO_2 (wt %) in isopropanol) were used as SiO_2 nanoparticles. Besides, 3-(methacryloyloxypropyl)trimethoxysilane (MPTS) (Abcr, 98%) and 3-(methacryloyloxypropyl)triethoxysilane (MPTES) (Abcr, 97%) were utilized as grafting agents. All chemicals were used without further purifications.

Synthesis of PMMA/SiO_2 Hybrid Nanocomposites

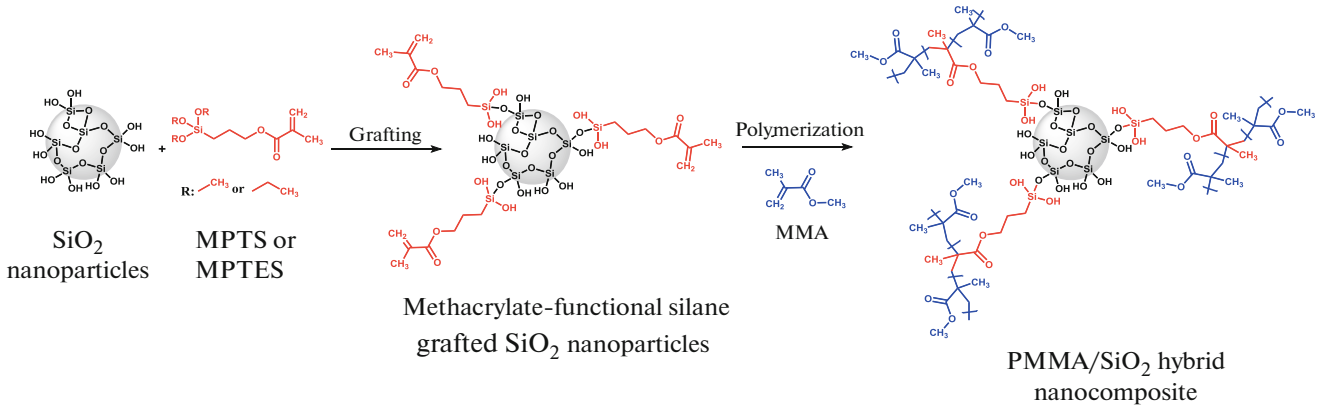
The synthesis of PMMA/SiO_2 hybrid nanocomposites has been realized in two reaction stages (Scheme 1). Firstly, two SiO_2 nanoparticles have been grafted by using different grafting agents; MPTS, 6 wt % and MPTES, 7.2 wt % of solid SiO_2 nanoparticles. Briefly, colloidal silica was placed into the reaction flask and then grafting agents were added dropwise during stirring at 500 rpm, and this blend continued to be stirred for about 30 min at room temperature. In the second stage, the polymerization of MMA has been carried out with the presence of thermal initiator (BPO, 2 wt % of MMA). Then, MMA and BPO were added into the prepared solution, which included grafted colloidal silica, and stirred for 15 min at room temperature. This final dispersion was fed with argon gas, afterwards, the reaction flask was covered with rubber cap. At the end, the polymerization reaction was completed by keeping the reaction flask at 75°C for 24 h. Eventually, resulting synthesized materials included various amount of SiO_2 ranged from 0 to 20 wt %.

Characterization

Fourier transform infrared (FTIR) spectroscopy (TENSOR 27) in transmission mode ranging from 400 to 4000 cm^{-1} at a resolution of 4 cm^{-1} was performed. Transmittance spectra of monomer and hybrid solutions were recorded by using a Horizontal Attenuated Total Reflectance (HATR) device. After polymerization, obtained PMMA/SiO_2hybrid nanocomposites were analyzed by using KBr pellet technique.

Thermal analysis was conducted by using Differential Scanning Calorimetry (DSC) (Perkin Elmer DSC7) to determine the glass transmission temperatures T_g of PMMA/SiO_2 hybrid nanocomposites. The measurement was performed with a rate of 20 grad/min and a temperature range of 20–370°C in a nitrogen atmosphere.

In order to investigate the degradation characteristics of PMMA/SiO_2 hybrid nanocomposites, Thermogravimetric analysis (TGA) was carried out by uti-



Scheme 1.

lizing Seiko SII TG/DTA 7200 thermogravimetric analyzer. The tests were run from 30 to 600°C with a heating rate of 10 K/min under ambient atmosphere.

The morphological properties of the PMMA/SiO_2 hybrid nanocomposites were examined by Scanning Electron Microscopy (SEM) by FEI, Quanta 200 FEG. Elemental composition of hybrid nanocomposites was analyzed by using energy dispersive X-ray detector (EDS).

RESULTS AND DISCUSSION

FTIR Analysis

According to FTIR spectra in Fig. 1, it has been approved that thermal polymerization of MMA and MMA blends have been occurred. Before polymerization which is represented in Fig. 2a, the standard peaks appeared at 1720 and 1635 cm^{-1} belonged to carbonyl (C=O) stretching vibration and C=C stretching, respectively [31–33]. The asymmetric C–H stretching, asymmetric C–H bending and symmetric C–H bending of the methyl group ($C-CH_3$) have been observed at 2955, 1443, and 1380 cm^{-1}, subsequently. Furthermore, the C–H stretching of $C=CH_2$ group appeared at 3100 cm^{-1} [34–36]. On the other hand, it has been observed that after the polymerization, the intensities of the related C=O and C=C peaks diminished noticeably. Moreover, C–H stretching of $C=CH_2$ group has been disappeared and C=O peak at 1720 cm^{-1} shifted slightly to 1730 cm^{-1} after polymerization. Also, when $SiO_2$was introduced to the blend, the characteristic peaks mentioned above remained the same, however, the broad peak was seen between 3400 and 3200 cm^{-1} due to the stretching vibrations of the hydrogen bonding of O–H groups on the surface of SiO_2 nanoparticles.In addition, when $SiO_2$was grafted with MPTS and MPTES and interacted with MMA, there was no different specific peak has been observed (Fig. 1b). According to the obtained results, FTIR analysis confirmed that the polymer structure was formed successfully.

DSC Analysis

Table 1 illustrates the alterations of T_g results of pristine PMMA and PMMA/SiO_2 hybrid nanocomposites with 20% ungrafted silica (20% SiO_2-PMMA) and various contents of grafted silica nanoparticles. According to the findings, T_g value of the pristine PMMA has been measured as 103°C, however, the addition of ungrafted silica nanoparticles into the blend, the T_g value increased notably to 121°C which is most probably due to the specific role of hydroxyl groups on the surface of silica nanoparticles that increased the physical interactions within the polymer matrix and reduced the chain mobility [20–22, 37]. In the case of PMMA/SiO_2 hybrid nanocomposites containing MPTS grafted silica nanoparticles, different T_g values have been obtained which was influenced by the various amount (5–20 wt %) of the particles in the blend. Results proved that the highest T_g value (149°C) was belonged to the hybrid nanocomposite that included 20 wt % of MPTS grafted silica nanoparticles (MPTS@20% SiO_2-PMMA) in it. On the other hand, introducing 15 and 20 wt % of MPTES grafted silica nanoparticles into the blend had greater impact on the T_g values which were recorded as 159°C for MPTES@15% SiO_2-PMMA and 166°C for MPTES@20% SiO_2-PMMA, respectively. In overall, it can be stated that grafted nanoparticles created some sort of synergistic affect since the compatibility between the polymer matrix and nanoparticles enhanced through the cross-linkings of acrylate groups (Scheme 1). As a result, the movement of polymer chains was restrained because of the improved interaction of PMMA network. Therefore, the thermal stability of the hybrid nanocomposite was mounted and the T_g increased [29]. To emphasize the difference between the performances of MPTS and MPTES regarding increasing the T_g value, it could be

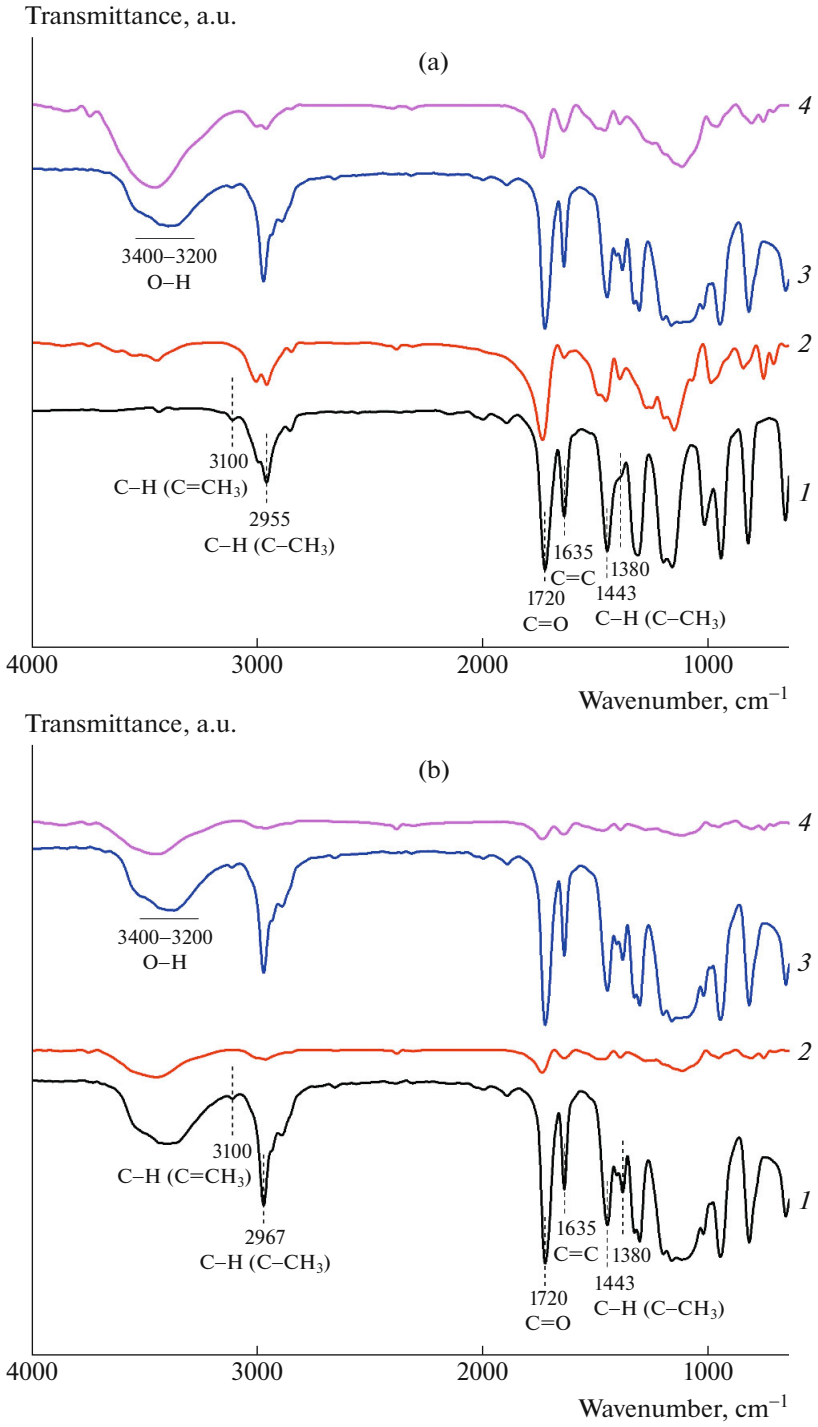


Fig. 1. FTIR spectra of (a) (*1*) MMA, (*2*) PMMA, (*3*) 20% SiO_2+MMA and (*4*) 20% SiO_2-PMMA, (b) (*1*) MPTS@20% SiO_2+MMA, (*2*) MPTS@20% SiO_2-PMMA, (*3*) MPTES@20% SiO_2+MMA and (*4*) MPTES@20% SiO_2-PMMA.

expressed that this situation is dependent on the homogeneity level of grafting process of nanoparticles surfaces. To our opinion, the grafting agent that possessed ethoxy groups ($-OCH_2CH_3$) enabled better homogenous grafting process comparing with the agent that had methoxy groups ($-OCH_3$). The reason behind this theory is due to the hydrolysis rate of $-OCH_3$ which 6–10 times higher than $-OCH_2CH_3$ [38]. For deeper explanation, during the grafting process, rapid hydrolysis of MPTS causes self-condensation of MPTS molecules and this hinder the homogenous grafting process of silica nanoparticles surfaces.

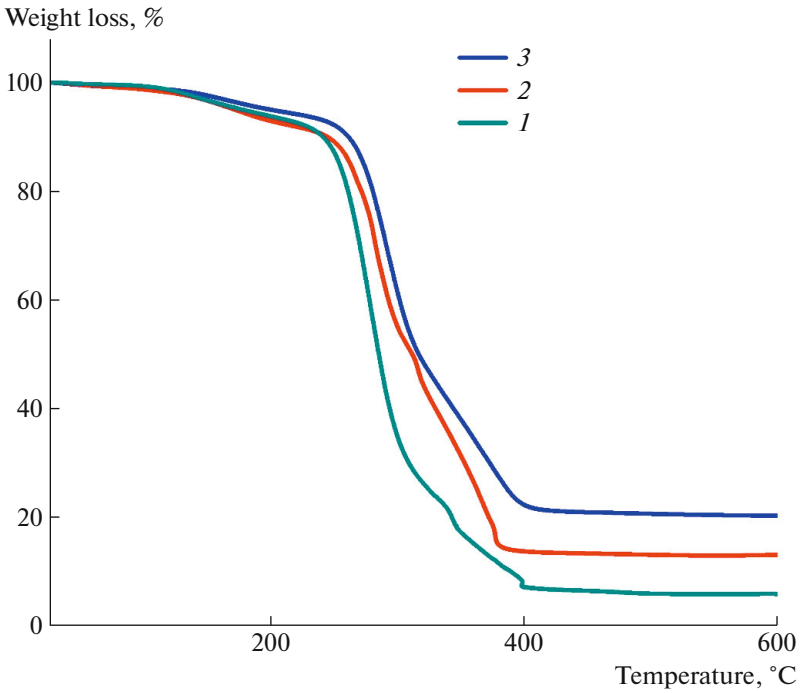


Fig. 2. TGA thermograms of (*1*) PMMA, (*2*) 20% SiO_2-PMMA and (*3*) MPTES@20% SiO_2-PMMA.

TGA Analysis

In order to explore the thermal degradation characteristics of PMMA/SiO_2 hybrid nanocomposites, TGA analysis was conducted for three comparable samples; PMMA, 20% SiO_2-PMMA and MPTES@20% SiO_2-PMMA hybrid nanocomposites (Fig. 2). In the literature, it was reported that neat PMMA decomposition occurs in three stages. According to this information, firstly, weakest linkage (H–H) in the oligomers starts to decompose. Secondly, retained monomers, which are not attended to the polymerization, degrade. Lastly, most stable linkages of saturated oligomer decompose [39–41]. Our results have almost been correlated with the literature. As it can be clearly identified from the TGA curves in Fig. 3 that for all samples, an initial mass loss around 3.3% for PMMA and 20% SiO_2-PMMA, and 2.3% for MPTES@20% SiO_2-PMMA have been recorded up to a temperature of 150°C which was associated with the existed adsorbed moisture. In the next phase, degradation of samples started at around 238°C for PMMA and at approximately 255°C for 20% SiO_2-PMMA and MPTES@20% SiO_2-PMMA. Major thermal decomposition for all nanocomposites began at around 300°C and completed at almost 400°C. Mass loss differences between 150 and 600°C have been calculated as 90.6, 83.3 and 77.3% for PMMA, 20% SiO_2-PMMA and MPTES@20% SiO_2-PMMA, respectively. Findings revealed that thermal stabilities of nanocomposites were improved as ungrafted and grafted silica nanoparticles were incorporated into the PMMA.

SEM-EDS Analysis

Figure 3 illustrates the SEM and EDS images of PMMA, 20% SiO_2-PMMA and MPTES@20% SiO_2-PMMA hybrid nanocomposites. When the SEM micrographs are examined carefully, it is obvious that there have been meaningful alterations among the samples in terms of morphology and material homogeneity. Figures 3a and 3d pointed out homogenous structure of PMMA. On the contrary, it is clear that the image belongs to 20% SiO_2-PMMA (Figs. 3b, 3e) exhibits that when ungrafted silica nanoparticles were

Table 1. Thermal properties of PMMA and PMMA/SiO_2 hybrid nanocomposites

Samples	Grafting Agent	SiO_2, %	T_g, °C
PMMA	–	–	103
20% SiO_2-PMMA	–	20	121
MPTS@5% SiO_2-PMMA	MPTS	5	118
MPTS@10% SiO_2-PMMA		10	116
MPTS@15% SiO_2-PMMA		15	136
MPTS@20% SiO_2-PMMA		20	149
MPTES@5% SiO_2-PMMA	MPTES	5	110
MPTES@10% SiO_2-PMMA		10	121
MPTES@15% SiO_2-PMMA		15	159
MPTES@20% SiO_2-PMMA		20	166

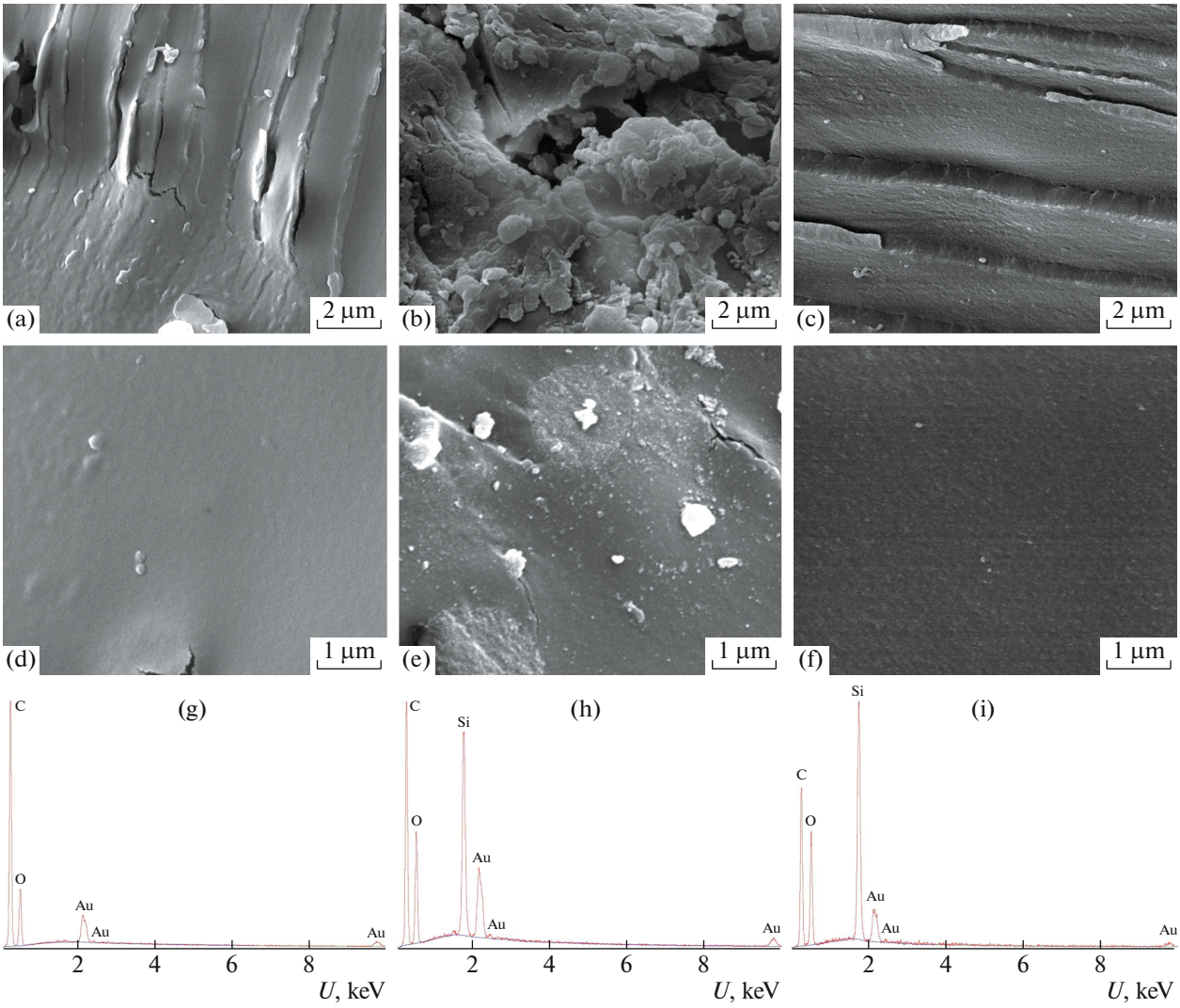


Fig. 3. SEM micrographs of samples observed at different magnifications. (a) PMMA 25000×, (b) 20% SiO_2-PMMA 25000×, (c) MPTES@20% SiO_2-PMMA 25000×, (d) PMMA 50000×, (e) 20% SiO_2-PMMA 50000×, (f) MPTES@20% SiO_2-PMMA 50000×; EDS images of samples: (g) PMMA, (h) 20% SiO_2-PMMA, (i) MPTES@20% SiO_2-PMMA.

incorporated into PMMA, surface smoothness was worsened and heterogeneous nanocomposite structure was obtained due to local dispersion of nanoparticles in the polymer phase which entailed large aggregations. On the other hand, for MPTES@20% SiO_2-PMMA hybrid nanocomposite (Figs. 3c, 3f), it is evident that surface morphology and material integrity were improved because the existence of acrylate groups on the surface of silica particles hampered the aggregation, as a result, more homogenous and effective dispersion of nanoparticles was realized in the PMMA matrix.

EDS microanalysis on the selected region depicts the PMMA consists of primarily C and O elements (Fig. 3g). In addition, Figs. 3h and 3i confirm the existence of Si in both 20% SiO_2-PMMA and MPTES@20% SiO_2-PMMA hybrid nanocomposites.

CONCLUSIONS

This work considered to prepare PMMA/SiO_2 hybrid nanocomposites and explored the impact of ungrafted and grafted silica nanoparticles on the T_g values as well as the structural properties of the yielded nanocomposites. Experimental procedures proved that thermal polymerization of MMA and MMA blends have been realized. Also, the addition of ungrafted and grafted nanoparticles into the polymer matrix increased T_g values, however, the increase was the greater for MPTES@20% SiO_2-PMMA comparing with the other nanocomposites due to the amount of silica nanoparticles as well as ethoxy groups ($-OCH_2CH_3$) enabled better homogenous grafting process. Findings revealed that thermal stabilities of nanocomposites were enhanced as ungrafted and

grafted silica nanoparticles were introduced to the PMMA. Furthermore, SEM results verified that surface morphology and material integrity were improved for MPTES@20% SiO_2-PMMA hybrid nanocomposite.

ACKNOWLEDGMENTS

Authors would like to thank to Prof. Dr. Turgay Seçkin at Chemistry Department of İnönü University for his technical support for TGA analysis.

CONFLICT OF INTEREST

The authors declared that they have no conflict of interest.

REFERENCES

1. D. Abliz, Y. Duan, L. Steuernagel, L. Xie, D. Li, and G. Ziegmann, Polym. Compos. **21**, 341 (2013).
2. M. H. Naveen, N. G. Gurudatt, and Y.-B. Shim, Appl. Mater. Today **9**, 419 (2017).
3. M. Dziadek, E. Stodolak-Zych, and K. Cholewa-Kowalska, Mater. Sci. Eng., C **71**, 1175 (2017).
4. L. Liu, D. Ye, R. Dong, D. Chen, S. Li, K. Cao, G. Cheng, S. Chen, and W. Huang, ACS Appl. Energy Mater. **3**, 4068 (2020).
5. B. H. Patel and P. V. Joshi, J. Packag. Technol. Res. **4**, 95 (2020).
6. H. Abbas, S. Iqbal, S. Ahmad, and N. Arfin, Mater. Res. Express **5** (8), 085312 (2018).
7. S. Rattan, P. Singhal, and A. L. Verma, Polym. Eng. Sci. **53**, 2045 (2013).
8. T. Lin and Y. Zheng, Micro Nano Lett. **8**, 217 (2013).
9. X. Song, X. Wang, H. Wang, W. Zhong, and Q. Du, Mater. Chem. Phys. **109**, 143 (2008).
10. V. I. Bykov, K. L. Makovetskii, D. S. Popov, M. V. Bermeshev, T. A. Butenko, and Yu. A. Talyzenkov, Dokl. Chem. **439**, 227 (2011).
11. P. Xu, H. Wang, R. Tong, Q. Du, and W. Zhong, Colloid Polym. Sci. **284**, 755 (2006).
12. E. Arpac, S. Güven, Ş. Yılmaz, J. C. Schmidt, H. Schmidt, D. Mochizuki, and K. Osada, WO Patent No. WO/2009/115566 (2009).
13. P. Judeinstein and C. Sanchez, J. Mater. Chem. **6**, 511 (1996).
14. B. M. Novak, Adv. Mater. **5**, 422 (1993).
15. V. N. T. Satyanarayana Kuchibhatla, A.S. Karakoti, and S. Seal, JOM **57**, 52 (2005).
16. M. Iijima and H. Kamiya, KONA Powder Part. J. **27**, 119 (2009).
17. L. Guerrini, R. A. Alvarez-Puebla, and N. Pazos-Perez, Materials **11**, 1154 (2018).
18. H. Heinz, C. Pramanik, O. Heinz, Y. Ding, R. K. Mishra, D. Marchon, R. J. Flatt, I. Estrela-Lopis, J. Llop, S. Moya, and R. F. Ziolo, Surf. Sci. Rep. **72**, 1 (2017).
19. E. Yavuz, R. Erdem, E. Küçüksayan, E. Akarsu, and M. Akarsu, Fibers Polym. **22**, 1274 (2021).
20. N. Wang, X. Wu, and C. S. Liu, Polymers **11**, 979 (2019).
21. C. J. T. Landry, B. K. Coltrain, and B. K. Brady, Polymer **33**, 1486 (1992).
22. C. Li, J. Wu, J. Zhao, D. Zhao, and Q. Fan, Eur. Polym. J. **40**, 1807 (2004).
23. Y.-H. Hu, C.-Y. Chen, and C.-C. Wang, Polym. Degrad. Stab. **84**, 545 (2004).
24. M. Salami-Kalajahi, V. Haddadi-Asl, S. Rahimi-Razin, F. Behboodi-Sadabad, H. Roghani-Mamaqani, and M. Najafi, Int. J. Polym. Mater. **62**, 336 (2013).
25. W. Stöber, A. Fink, and E. Bohn, J. Colloid Interface Sci. **26**, 62 (1968).
26. Y. Lin, L. Liu, D. Zhang, Y. Liu, A. Guan, G. Wu, Soft Matter **12**, 8542 (2016).
27. Y. Yang and Y. Dan, Colloid Polym. Sci. **281**, 794 (2003).
28. M. Chen, L. Wu, S. Zhou, and B. You, Macromolecules **37**, 9613 (2004).
29. R. Y. Hong, H. P. Fu, Y. J. Zhang, L. Liu, J. Wang, H. Z. Li, and Y. Zheng, J. Appl. Polym. Sci. **105**, 2176 (2007).
30. J.-M. Yeh, C.-J. Weng, W.-J. Liao, and Y.-W. Mau, Surf. Coat. Technol. **201**, 1788 (2006).
31. Rd. S. Leão, S. L. D. de Moraes, K. A. S. Aquino, C. P. Isolan, B. Gd. S. Casado, and M. A. J. R. Montes, Int. J. Dent. 2**018**, 5743840 (2018).
32. A. R. Cho and S.-Y. Park, Opt. Mater. Express **5**, 690 (2015).
33. M. L. Saladino, T. E. Motaung, A. S. Luyt, A. Spinella, G. Nasillo, and E. Caponetti, Polym. Degrad. Stab. **97**, 452 (2012).
34. J. Coates, "Interpretation of Infrared Spectra, A Practical Approach," in *Encyclopedia of Analytical Chemistry: Applications, Theory and Instrumentation* (Wiley, New York, 2006). https://doi.org/10.1002/9780470027318.a5606
35. P. J. Launer and B. Arkles, "Infrared Analysıs of Organosılıcon Compounds: Spectra-Structure Correlatıons," in *Silicon Compounds: Silanes and Silicones* (Gelest, Inc Morrisville, PA, 2003), pp. 175–178.
36. B. H. Stuart, *Infrared Spectroscopy: Fundamentals and Applications* (John Wiley and Sons Ltd, West Sussex, England, 2004), pp.123–129.
37. Y. Lin, L. Liu, G. Xu, D. Zhang, A. Guan, and G. Wu, J. Phys. Chem. **119**, 12956 (2015).
38. B. Arkles, J. R. Steinmetz, J. Zazyczny, and P. Mehta, J. Adhes. Sci. Technol. **6**, 193 (1992).
39. T. Kashiwagi, A. Inaba, J. E. Brown, K. Hatada, T. Kitayama, and E. Masuda, Macromolecules **19**, 2160 (1986).
40. J. Rychlý and J. Pavlinec, Polym. Degrad. Stab. **28**, 1 (1990).
41. S. M. Lomakin, J. E. Brown, R. S. Breese, and M. R. Nyden, Polym. Degrad. Stab. **41**, 229 (1993).